

THE STATIC STRENGTH ANALYSIS OF FRICTION STIR WELDED STIFFENED PANELS FOR PRIMARY FUSELAGE STRUCTURE

A Murphy, F Lynch, M Price, P Wang

School of Aeronautical Engineering, Queen's University Belfast, Belfast, N. Ireland

Keywords: *friction stir welding, stiffened panels, crippling analysis, finite element analysis*

Abstract

The introduction of friction stir welding as an alternative joining process to riveting in the manufacture of primary aircraft structure has the potential to realise reductions in both manufacturing costs and structural weight. However, before this process can be applied commercially many issues need to be addressed. Methods for static strength analysis and design must be developed. This naturally involves the development and validation of analysis procedures for both the local buckling and post buckling behaviour of stiffened panels. This paper reports on the work undertaken to develop and validate analysis procedures for the crippling failure of welded skin-stringer sub-components. The experimental programme has demonstrated the potential static strength of skin-stringer friction stir welded joints. For each specimen tested, weld joint integrity was maintained throughout local skin buckling, post buckling and overall crippling. The work undertaken has demonstrated that the crippling behaviour of friction stir welded stiffened panel may be analysed considering standard buckling behaviour. However, standard stiffened panel buckling analysis procedures must be altered to account for the weld joint geometry.

1 Introduction

A typical aircraft fuselage is a stiffened shell structure, consisting of an external skin, stiffened by longitudinal stringer and lateral frame stiffeners. For current designs the skin, stringer and frame components are riveted

together, requiring thousands of rivets and hundreds of man or machine hours. With increasing demands from commercial carriers for reductions in aircraft acquisition costs along with increased performance, aircraft manufacturers are now required to consider advanced joining technologies for use on future programmes.

The introduction of welding as an alternative joining process to riveting in the manufacture of stiffened panels has the potential to realise reductions in both manufacturing time and costs [1]. The laser welding process can proceed at a rate of up to 10 m per minute compared to 0.1 m per minute for conventional auto riveting [2]. The manufacturing costs are consequently estimated to be in the region of 25% lower [3] and the introduction of advanced joining techniques has the potential of producing lighter structures due to the optimal placement of structural material and the elimination of joints and joint fasteners. Although this potential is recognised there are still issues to be addressed in particular surrounding weldability of standard materials and weld flaws, which can initiate cracks and correspondingly reduce fatigue life [4]. In addition, the potential manufacturing cost saving in terms of time may be outweighed by the increase in material costs currently required for laser beam welding.

An alternative joining process that removes the need for expensive non-standard material types is friction stir welding [5]. The friction stir welding process is a solid state joining technique. The process utilizes local friction heating to produce continuous solid-state seams.

The process joins materials by plasticising and then consolidating the material around the weld line. A cylindrical, shouldered tool with a profiled probe or pin is rotated and slowly plunged into the workpiece at the start of the weld line. The probe continues rotating and traverses forward in the direction of welding. Frictional heat is generated between the wear resistant tool and the material of the workpiece. As the probe proceeds, the friction heats the surrounding material and rapidly produces a plasticised zone around the probe. This heat causes the workpiece to soften at a temperature below that of the material melting temperature and typically within the material's forging temperature range. As the tool moves forward metal flows to the back of the tool where it is extruded/forged behind the tool. It then consolidates and cools to form the bond. To produce a full-penetration groove weld in a butt joint, the bottom of the tool must be close to the bottom of the workpiece. In order to make a lap joint, the bottom of the tool must only extend through the bottom of the top sheet and into the bottom sheet, creating a metallic bond between the two sheets. A schematic drawing of the lap joint welding process is shown in Figure 1. The weld is left in a fine-grained, hot-worked condition with no entrapped oxides or gas porosity. A benefit of this welding process is that it allows welds to be made on standard aircraft production aluminium alloys, which cannot be readily laser beam welded. In addition, friction stir welding is a robust, process tolerant technique. It has the advantage that many of the welding parameters, e.g. tool design, rotation speed and translation speed, can be controlled in a precise manner, thus controlling the energy input into the system [6]. The process also requires less stringent weld preparation.

Friction stir defect-free welds with good mechanical properties have been made in a wide variety of aluminium alloys, including some which were previously thought to be "unweldable". Butt welds have been produced in plates less than 1 mm thick and in plates more than 75 mm thick [7, 8]. A serious problem with fusion welding, even when a

sound weld can be made, is the complete alteration of microstructure and the accompanying loss of mechanical properties. Being a solid-state process, friction stir welding has the potential to avoid significant changes in both the microstructure and the mechanical properties [9].

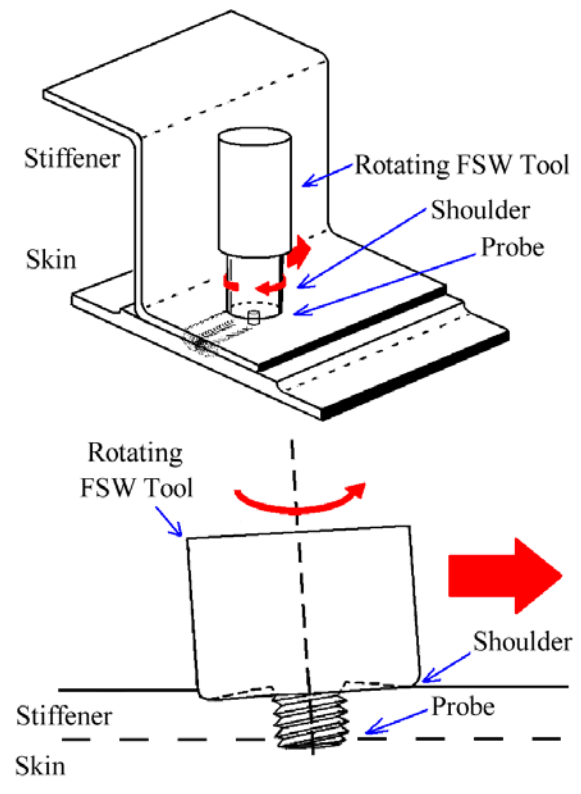


Fig. 1. Lap joint friction stir welding

The basic metallurgy in friction stir lap welds is similar to full penetration butt welds [10]. The weld joint includes a Thermo-Mechanically Affected Zone (TMAZ) and a Heat Affected Zone (HAZ), Figure 2. The Nugget region within the TMAZ and a region at the top of the weld (the crown) consist of very fine, recrystallised grains. These regions have experienced high temperatures and extensive plastic deformation and contain much smaller grains than the base metal. Within the remaining TMAZ the base metal grains have undergone some deformation; however, due to the lesser degree of deformation and lower temperatures experienced, recrystallisation will not have taken place. Adjacent to the TMAZ is the HAZ,

similar to that in fusion welding. The transitions from the TMAZ to the HAZ and from the HAZ to the base material are gradual and not distinguished by any abrupt change in microstructure [11]. In lap joint welding, the movement of material within the weld is more important than the microstructure developed [12]. The key to a sound joint is the transport of material around the tool probe which results in vertical transport of material in the longitudinal axis of the weld and hence the generation of a structural joint [7].

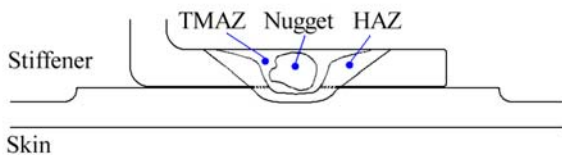


Fig. 2. Schematic of a typical transverse cross-section of a FSW lap joint

This article presents development work on potential analysis methods for the static strength of friction stir welded stiffened panel structure. The work assesses conventional analysis methods and potential Finite Element (FE) analysis methods for the crippling strength analysis of welded skin-stringer joints. The analysis work is validated on a single stiffener crippling specimen design, with a Z-section stringer stiffener (7075-T76511 extrusion) and a flat skin base (2024-T3). The specimen skin thickness and stringer dimensions are representative of panel structure found on the lower fuselage belly of mid-sized commercial transport aircraft, Figure 3.

The following section outlines the conventional analysis of the crippling specimen. This is followed by details of the computational static strength analysis. The validation experimental set-up is then introduced before the analytical, numerical and experimental results are presented and compared. Finally, the paper concludes by assessing the accuracy of the potential analysis methods for friction stir welded stiffened panels.

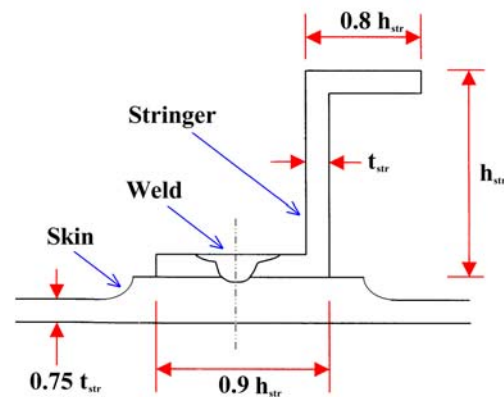
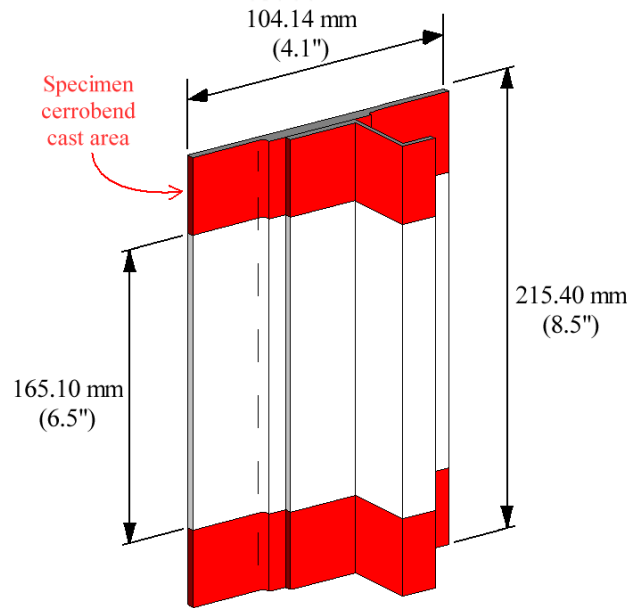


Fig. 3. Crippling specimen geometry

2 Conventional Analysis

The analysis methods applied to the welded panel are based on conventional aerospace panel analysis procedures. The local skin buckling and panel crippling analysis techniques are based on the methods presented in Bruhn [12], NASA Astronautics Structures Manual [13] and the ESDU Structures Sub-series [14]. At this stage the standard analysis methods were not modified to account for the effects of the welding process on structure's material properties.

The stress in the skin at which local buckling occurs is given by:

$$\sigma_{b(sk)} = \frac{k\pi^2 E_{t(sk)}}{12(1-\nu^2)} \left(\frac{t_{(sk)}}{b_{(sk)}} \right)^2 \quad (1)$$

The specimen skin segments are assumed to be fully clamped along the loading edges at the edge of the cerrobends cast supports and free at the specimen edge, the skin is conservatively assumed to be simply supported along the edge of the skin-stringer weld. $E_{t(sk)}$ is the tangent modulus of the skin material at $\sigma_{b(sk)}$ (which is used to account for plasticity). Using a Ramberg-Osgood fit the tangent modulus at a stress σ is given by:

$$E_t = E \left[1 + \left(\frac{\sigma}{\sigma_n} \right)^{m-1} \right]^{-1} \quad (2)$$

where E , m and σ_n are determined from material property tests carried out on the skin and stringer parent material prior to welding. In order to determine the failure load of the panel the crippling stresses of the stringer elements must first be determined. These stresses are derived from the local buckling stresses of the stringer web and flanges. For each stringer element the local buckling stress is given by:

$$\sigma_{b(elm)} = \frac{k\pi^2 E_{t(str)}}{12(1-\nu^2)} \left(\frac{t_{(elm)}}{b_{(elm)}} \right)^2 \quad (3)$$

k is dependant on the edge support conditions of the element.

In order to account for the welded skin-stringer joint three different crippling analysis idealisations were considered, Table 1.

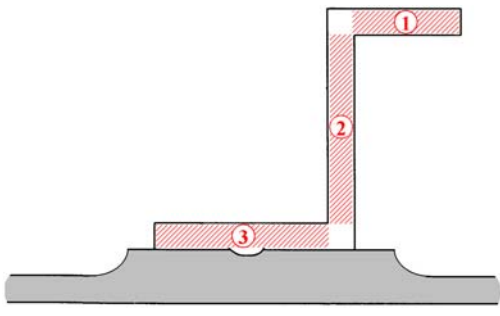
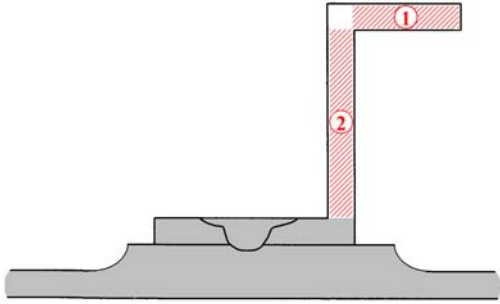
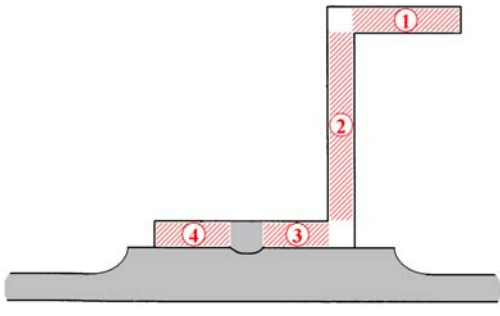
<p>Crippling Analysis A</p> <p>Weld joint ignored with the stiffener analysed as three crippling elements (equivalent to a riveted structure analysis):</p> <ul style="list-style-type: none"> • Element 1 has one edge simply supported and one edge free, $k=0.64$. • Element 2 has both edges simply supported, $k=4.0$. • Element 3 has one edge simply supported and one edge free, $k=0.64$. 	
<p>Crippling Analysis B</p> <p>The stringer is assumed to have only two crippling elements, with the attached flange assumed to acts with the effective specimen skin (equivalent to an integral structure analysis):</p> <ul style="list-style-type: none"> • Element 1 has one edge simply supported and one edge free, $k=0.64$. • Element 2 has both edges simply supported, $k=4.0$. 	
<p>Crippling Analysis C</p> <p>The stringer is divided into four crippling elements with the weld area assumed to acts with the effective specimen skin:</p> <ul style="list-style-type: none"> • Element 1 has one edge simply supported and one edge free, $k=0.64$. • Element 2 has both edges simply supported, $k=4.0$. • Element 3 has both edges simply supported, $k=4.0$. • Element 4 has one edge simply supported and one edge free, $k=0.64$. 	

Table. 1. Conventional crippling analysis idealisation

The flange and web crippling stresses, $\sigma_{c(elm)}$, are calculated from the corresponding local buckling stresses and the material compressive yield stress:

$$\sigma_{c(elm)} = \sqrt{\sigma_{b(elm)}\sigma_{cy}} \quad (4)$$

Finally, to determine the failure load of the panel the crippling stresses of the stringer is determined:

$$\sigma_{c(str)} = \frac{\sum b_n t_n \sigma_{c(elm)}}{\sum b_n t_n} \quad (5)$$

3 Computational Analysis

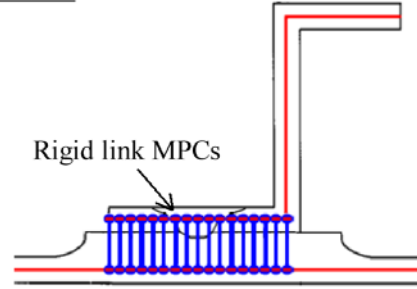
Considering the uncertainty surrounding the application of conventional crippling analysis methods, a finite element study on the crippling response of the specimens was undertaken. Using the finite element method and employing non-linear material and geometric analysis procedures, it is possible to model the post buckling behaviour of stiffened panels without having to place the same emphases on structural idealisation or empirical analysis methods.

3.1 Model Idealisation

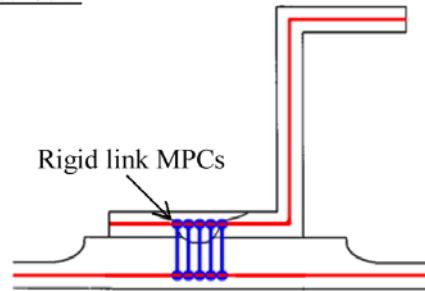
The idealisation approach adopted represents the stringer web and flanges and the specimen skin as an assemblage of shell elements. This approach is essential to enable the crippling failure modes of the structure to be simulated. A number of idealisations for the skin-stringer weld joint were examined, Figure 4. In Method 1 the specimen is assumed to act as an integral structure with all nodes on the stringer flange connected to the corresponding skin nodes, Figure 4. In Method 2 the weld joint is explicitly modelled, with nodes in the skin and stringer weld area connected with rigid links, Figure 4. Method 2 does not model the contact condition between the unwelded skin and stringer flange and therefore within the post-buckling domain the skin and flange shells may penetrate each other. Method 3 therefore models the weld plus the skin and flange interface

contact conditions. This is accomplished in ABAQUS with the remaining nodes at the interface linked using uni-axial gap elements, GAPUNI [15].

Method 1



Method 2



Method 3

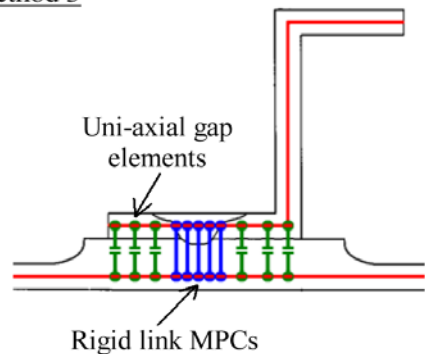


Fig. 4. Skin-stringer interface idealisation

3.2 Element Selection

To enable element selection a series of mesh convergence studies were undertaken. The buckling behaviour of uniformly compressed rectangular plates with geometries and boundary conditions designed to replicate those of the specimen's individual plate segments were carried out. Each analysis set was developed such that a theoretical buckling calculation could be preformed [16]. The performance of

five ABAQUS elements were assessed based on convergence with corresponding theoretical behaviour with increasing mesh densities. Based on these analyses the first-order curved quadrilateral 4-noded finite strain general-purpose shell element, S4R [15] was selected along with the mesh illustrated in Figure 5.

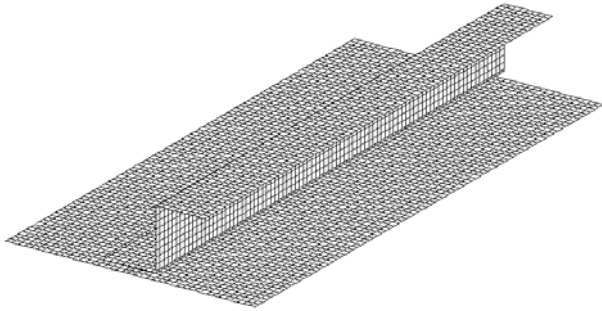


Fig. 5. Specimen mesh (Method 2)

3.3 Material Modelling

Compressive parent material properties obtained from coupon tests were used in all Finite Element analysis. Material test coupons were taken from the same material batches as the components from which the specimens were manufactured. Material curves were incorporated into the Finite Element analysis models using the ‘classical metal plasticity’ constitutive theory available within the ABAQUS material library [15]. At this stage the potential degradation of material properties due to the welding process have not been considered.

3.4 Loads and Boundary Conditions

The loads and boundary conditions applied to the models were designed to be as representative of the experimental test setup as possible, with the same loading and boundary conditions applied to each model. A uniform axial displacement was applied to one end of the model with the axial displacement at the opposite end restrained. Out-of-plane displacements of the nodes within the areas that were cast in Cerrobend in the experimental test were restrained.

3.5 Solution Procedure

For each analysis model an initial eigenvalue analysis is performed to determine the fundamental buckling mode of the structure. The initial geometry is subsequently seeded with an imperfection in the shape of the fundamental buckling mode. Unless otherwise stated, the magnitude of this imperfection is 10% of the skin thickness, a value that is representative of typical imperfections present in conventional riveted fuselage structures. The non-linear post buckling analysis is then performed using the incremental-iterative Newton-Raphson solution procedure [17].

4 Validation Testing

This section outlines the experimental work carried out to validate the accuracy of the proposed conventional crippling analysis methods and the finite element methods. The welded specimens consisted of a 104 mm by 165 mm flat skin, stiffened by a single Z-section extruded stringer, as shown in Figure 3. The specimens were tested in a 250 kN capacity hydraulic, load-controlled compression-testing machine. A 25.4 mm thick Cerrobend (low melting point alloy) base was cast on to the specimens, producing fully clamped boundary conditions at each end. Keying holes were drilled through the ends of the specimens prior to casting to hold the Cerrobend in position and to help prevent separation of the Cerrobend from the specimen. The ends were subsequently machined flat and perpendicular to the skin to ensure that uniform axial loads were applied. Two LVDTs, one either side of the specimen, were used to measure specimen end-shortening. One specimen was strain gauged to determine buckling behaviour. The specimens was loaded monotonically at a rate of approximately 10 kN/min until failure occurred, end-shortening and strain data were recorded automatically at 4-second intervals.

5 Results and Discussion

5.1 Local Skin Buckling

The conventional analysis predicted local skin buckling loads and finite element predicted local skin buckling loads and modes are presented in Table 2. The values are presented as percentages of the experimental measured local skin buckling load. Test specimen 2 was strained gauged to determine local skin buckling behaviour. The specimen skin initially buckled in ‘Mode 1 (-)’, Figure 6, before mode jumping into ‘Mode 2(+/-)’ at 349% the initial buckling load. Examining the conventional analysis predictions, clearly the assumption that the skin is simply supported along the edge of the skin-stringer weld is conservative. The true support conditions along the weld line lie between simple support and fully fixed and are dependant on the complex interaction of the welded skin and stringer joint and the relative stiffness properties of the skin and stringer.

Considering the finite element predictions, all models appear to over predict specimen local buckling. FE Methods 2 and 3 give the closest predictions, over predicting the buckling load by approximately 14%. Idealising the skin-stringer joint as an integral structure, FE Method 1, increases this over prediction to almost 30%, indicating that this method of idealisation is not appropriate for this welded structure.

All three models predict an identical local skin buckling mode. This mode is similar to that observed in test specimen 1 and 3 but is different to that of specimen 2. The difference in experimental local buckling modes indicates that the structure is sensitive to initial imperfections. The assumption of an imperfection magnitude of 10% skin thickness was based on riveted structure allowable tolerances and not measured specimen imperfections. Based on theory [16] and clearly demonstrated in the literature [18-20], the modelling of initial geometric imperfections is of great importance when evaluating initial skin buckling behaviour. In addition, geometric imperfections typically occur as a result of residual stresses generated during

manufacturing, at this stage of development the finite element models do not represent welding induced residual stresses.

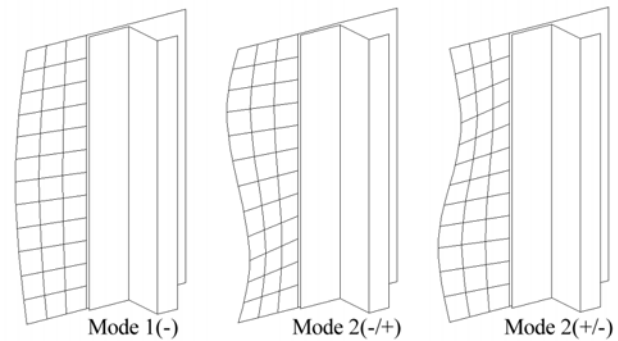


Fig. 6. Local skin buckling modes

5.2 Specimen Crippling

The conventional predicted specimen failure loads and the experimental and finite element predicted specimen failure loads and modes are presented in Table 3. The load versus end-shortening curves obtained from the finite element models are shown in Figure 7, together with the corresponding test and conventional crippling analysis results. As with the local buckling results, the values are presented as percentages of the experimental behaviour, percentages are based on the lower bound experimental failure load (Test specimen 2).

Considering first the experimental behaviour, all three specimens failed at load levels within 2.4% of each other. Test specimens 1 and 3 failed in crippling with the skin elements rotating anticlockwise and the stringer web and free flange elements rotating clockwise, in the top half of the specimen. Specimen 2 failed with the skin elements rotating clockwise and the stringer elements rotating anticlockwise, Figure 8. For all three specimens the skin-stringer weld remained intact into the specimen post failure region.

Examining the conventional crippling analysis methods, both analysis A and B over predict the failure strength of the structure. Clearly it is inappropriate to analyse the continuous welded joint structure as a discontinuous riveted type structure, Analysis A, nor is it appropriate to analyse the welded

skin stringer combination as an integral type structure, Analysis B. Analysing the welded skin-stringer structure assuming the attached flange acts as a series of small crippling

elements, Analysis C, offers the most appropriate analysis method as only this approach appears to conservatively predict the structural behaviour.

	Local skin buckling load as percentage experimental value* (%)	Local skin buckling mode
Test specimen 1	---	Mode 2(-/+)
Test specimen 2	100.0	Mode 1(-)
Test specimen 3	---	Mode 2(-/+)
Conventional analysis	55.7	---
FE Method 1, 10% Imp.	129.3	Mode 2(-/+)
FE Method 2, 10% Imp.	113.6	Mode 2(-/+)
FE Method 3, 10% Imp.	114.3	Mode 2(-/+)

Table 2. Local skin buckling loads (* based on Test specimen 2)

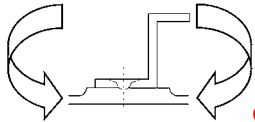
	Crippling failure load as percentage experimental value* (%)	Specimen crippling failure mode in the top half of the specimen
		
Test specimen 1	101.8	Skin elements rotated anticlockwise, stringer web and free flange elements rotated clockwise.
Test specimen 2	100.0	Skin elements rotated clockwise, stringer web and free flange elements rotated anticlockwise.
Test specimen 3	102.4	Skin elements rotated anticlockwise, stringer web and free flange elements rotated clockwise.
Crippling Analysis A	105.0	---
Crippling Analysis B	102.2	---
Crippling Analysis C	96.5	---
FE Method 1, 10% Imp.	109.2	Skin elements rotated clockwise, stringer web and free flange elements rotated anticlockwise.
FE Method 2, 10% Imp.	93.5	Skin elements rotated clockwise, stringer web and free flange elements rotated anticlockwise.
FE Method 3, 10% Imp.	98.9	Skin elements rotated clockwise, stringer web and free flange elements rotated anticlockwise.

Table 3. Crippling analysis loads (* based on Test specimen 2)

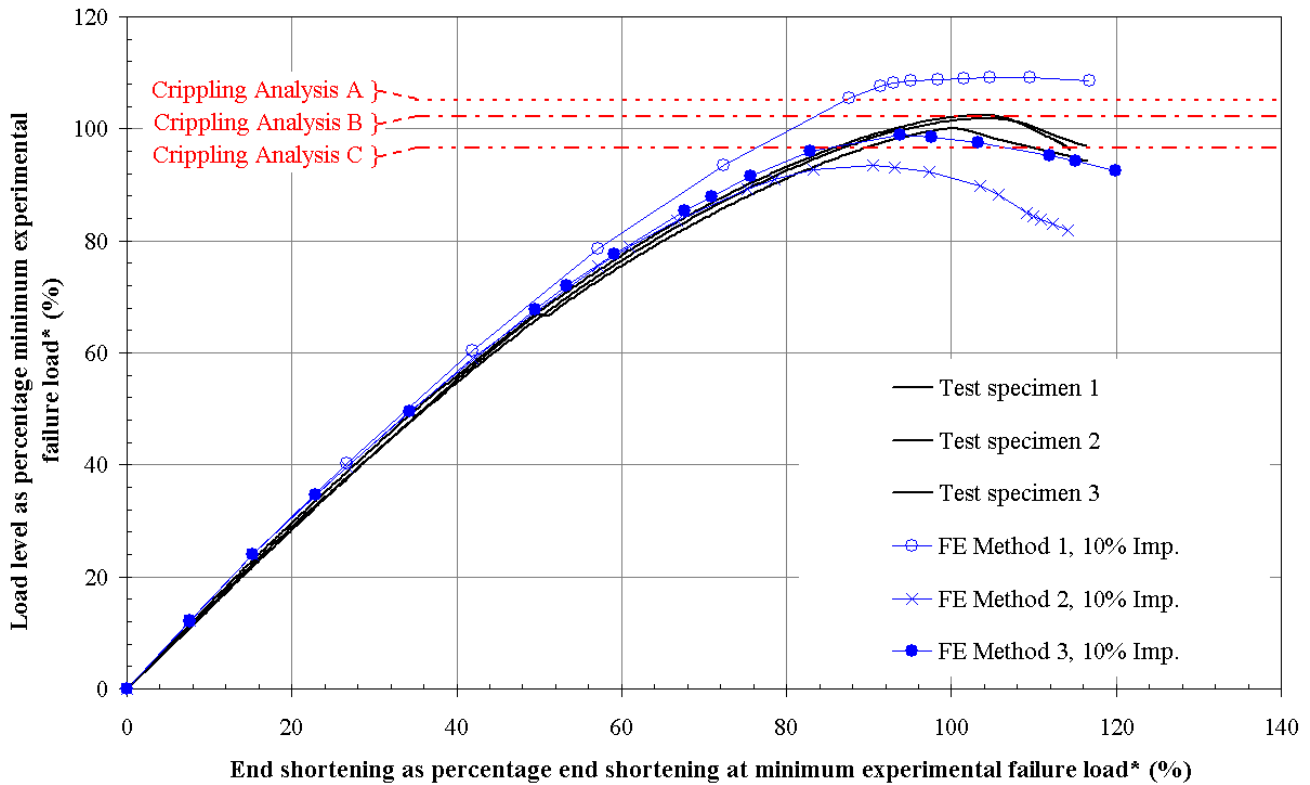


Fig. 7. FE and experimental load-deflection curves (* based on Test specimen 2)

Considering the finite element predictions, each model's predicted pre-buckling stiffness correlates well with the experimental behaviour, Figure 7. Again all three modelling methods result in the same predicted mode shape, this time with the skin elements rotated clockwise and the stringer web and free flange elements rotated anticlockwise in the top half of the specimen, Figure 8. Examining the post-buckling stiffness, clearly the integral idealisation, Method 1, results in an overly stiff model and ultimately an over prediction of the failure load of the structure. Studying idealisation Method 2, which does not consider the contact conditions between the skin and the stringer flange, results in an under prediction of the specimen's post-buckling stiffness and failure load. Idealising the skin-stringer joint considering contact behaviour, Method 3, most accurately represents the structural behaviour and results in an under prediction of 1.1%.

The finite element analysis results appear very accurate, however it is worth noting that the models do not, as yet represent the effects of

the welding process such as altered material properties or welding induced residual stresses.



Fig. 8. FE Method 3 predicted failure mode and test specimen 2 failure mode

6 Conclusions

The experimental programme has demonstrated the static strength of the friction stir welded skin-stringer joints. For each specimen tested, weld joint integrity was maintained throughout local skin buckling, post buckling, and ultimately overall specimen crippling. The experimental specimen behaviour establishes that friction stir welded stiffened panels may be designed considering standard crippling behaviour. However, standard stiffened panel buckling analysis procedures must be altered to account for the weld joint geometry. In addition, non-linear finite element analysis procedures may be used to accurately model the crippling behaviour, again the weld joint geometry must be accurately represented along with the contact conditions at the joint interface.

The methods developed and validated do not consider welding effects on material properties and resultant residual stresses. Further work is required to modify the finite element analysis procedures to consider material, geometry, and residual stress properties due to the friction stir welding process. The data and knowledge gained here, on the analysis of crippling skin-stringer joints, will be used in the design and testing of larger subcomponent demonstrator panels, as part of the next step on the road to the safe introduction of welded structure in aircraft production.

References

- [1] Irving P. End of the aircraft rivet-the coming of the welded aircraft. *Aerogram*, Vol. 10, No. 2, September 2001.
- [2] Gibson A. *An investigation into the compressive strength and stability characteristics of welded aircraft fuselage panels*. PhD Thesis, Queen's University Belfast, N. Ireland, 2000.
- [3] Zink W. Laser beam welding for aircraft structures. *Aeromat 2000*, Daimler Chrysler Aerospace Airbus, Bremen, 2000.
- [4] Pang H L J. Analysis of weld toe profiles and weld toe cracks. *International Journal of Fatigue*, Vol. 15, No. 1, pp. 31-36, 1993.
- [5] Midling O T. Material flow behaviour and microstructural integrity of friction stir butt weldments. *Proceedings of the 4th International Conference on Aluminium Alloys*, Atlanta, pp. 451-458, 1994.
- [6] Peel M, Steuwer A, Preuss M and Withers P J. Microstructure, mechanical properties and residual stresses as a function of welding speed in aluminium AA5083 friction stir welds. *Acta Materialia*, Vol. 51, pp. 4791-4801, 2003.
- [7] Colligan K. Material flow behaviour during friction stir welding of aluminum. *Welding Journal*, 78(7): 229-s to 237-s, 1999.
- [8] Thomas W M and Nicholas E D. Friction stir welding for the transportation industries. *Materials & Design*, Vol. 18, No. 4/6, pp. 269-273, 1997.
- [9] Rhodes C G, Mahoney M W, Bingel W H, Spurling R A and Bampton C C. Effects of friction stir welding on microstructure of 7075 aluminum. *Scripta Materialia*, Vol. 36. No.1. pp. 69-15, 1997.
- [10] Dracup B J and Arbogast W J. Friction stir welding as a rivet replacement technology. *Proceedings of the 1999 SAE Aerospace Automated Fastening Conference & Exposition*, Memphis, TN, October 5-7, 1999.
- [11] Lockwood W D, Tomaz B and Reynolds A P. Mechanical response of friction stir welded AA2024: experiment and modelling. *Materials Science and Engineering A*. 323(1-2): 348-353, 2002.
- [12] Bruhn E F. *Analysis and design of flight vehicle structures*. 1st edition, Tri-State Offset Company, 1973.
- [13] NASA, *NASA Astronautics structures manual*, Volume 3, NASA, Washington, US, 1961.
- [14] ESDU Structures sub-series, *Engineering Sciences Data Units*, ESDU International Ltd.
- [15] Anonymous. *ABAQUS / Standard user's manual*. Version 6.1, Hibbitt, Karlsson and Sorenson, 2000.
- [16] Bulson P S. *The stability of flat plates*, 1st edition, Chatto & Windus, London, 1970.
- [17] Becker A A. *Understanding non-linear finite element analysis - Through illustrative benchmarks*, 1st edition, NAFEMS (ISBN 1-8743-7635-2), 2001.
- [18] Lynch C J. *A finite element study of the post buckling behaviour of a typical aircraft fuselage panel*. PhD Thesis, Queen's University Belfast, N. Ireland, 2000.
- [19] Hu S Z and Jiang L. A Finite element simulation of the test procedure of stiffened panels. *Marine structures*, Volume 11 pp 75-99, 1998.
- [20] Baker D J and Kassapoglou C. Post buckled composite panels for helicopter fuselages: Design, analysis, fabrication and testing. *Presented at the American Helicopter Society*, Hampton roads chapter, structures specialists meeting, Williamsburg VA US, October 2001.